# ARTICLES

## Photodissociation of Unsaturated Alcohols. Energy Distribution in the Nascent OH Radicals

**Suresh Dhanya, Awadhesh Kumar, Hari P. Upadhyaya, Prakash D. Naik, and Rameshwar D. Saini***

*Radiation Chemistry and Chemical Dynamics Division, Bhabha Atomic Research Centre, Trombay, Mumbai-400 085, India*

*Received: May 31, 2004; In Final Form: July 22, 2004*

The photodissociation of allyl and propargyl alcohols at 193 nm, which involves $\pi-\pi^*$ electronic transition and leads to the formation of OH, has been studied by using a laser photolysis−laser-induced fluorescence technique. The nascent OH radicals formed from both these molecules are found to be rotationally and vibrationally excited. The vibrational distributions are found to be similar, described by vibrational temperatures of 2070 ± 380 and 2130 ± 440 K for allyl and propargyl alcohols, respectively. The rotational temperatures of both $v'' = 0$ and 1 levels of OH radicals from allyl alcohol are found to be almost the same, viz., 1960 ± 150 and 1900 ± 250 K, respectively, and close to the vibrational temperature. On the other hand, the rotational temperatures of OH radicals, 1760 ± 130 K at the $v'' = 0$ level and 690 ± 120 K at the $v'' = 1$ level, are very different from each other, in the case of propargyl alcohol. In both molecules, a significant part of the available energy is partitioned into the relative translational energy of the fragments, 118.4 ± 22.2 and 148.0 ± 23.0 kJ mol$^{-1}$ in allyl and propargyl alcohols, respectively. The results indicate a quantitative difference in the energy partitioning within the fragments of the two molecules, and only a hybrid model involving an exit barrier can explain the observations.

### Introduction

Recently, studies on photodissociation dynamics of small molecules belonging to different classes have been pursued intensely with the objective of understanding the details of initial excitation and bond dissociation, and predicting the same with the help of advanced theoretical calculations. While photodissociation of unsaturated molecules with a carbon − carbon double bond, such as allyl compounds ($CH_2$═$CH-CH_2X$), have been the subjects of several such studies,[1−4] investigations on propargyl compounds ($CH$≡$C-CH_2X$) with a carbon−carbon triple bond are limited to the identification and characterization of the propargyl radical spectrum.[5,6] Recently, we studied C−OH dissociation of unsaturated carboxylic acids, namely, acrylic acid ($CH_2$═$CH-COOH$),[7] and propiolic acid ($CH$≡$C-COOH$)[8] by a laser flash photolysis−laser-induced fluorescence technique and observed marked differences in the patterns of energy distribution among their fragments. While the major fraction (0.75) of the available energy goes as the translational energy of the fragments in the case of propiolic acid, the corresponding fraction is only 0.25 in acrylic acid. This prompted us to investigate the energy partitioning in C−OH dissociation in the corresponding alcohols, namely, acrylic ($CH_2$═$CH-CH_2OH$) and propargyl ($CH$≡$C-CH_2OH$) alcohols, and compare this with the energy distribution patterns observed in the case of acrylic and propiolic acids. Except for a laser flash photolysis study to detect the allyl radical[2] and an emission spectrum study supported by theoretical calculations to see the nature of the excited state of allyl alcohol,[4] there were no studies on the dynamics or the direct observation of the OH fragment in the photodissociation of these two molecules. Thus, the present study on allyl and propargyl alcohols, using laser-induced fluorescence as a probe for the OH fragment was initiated to see the energy distribution among the fragments, and the preliminary results were reported in a symposium.[9] Subsequently, we came across a very similar study on allyl alcohol by Kang et al,[10] whose results are in general agreement with our results on allyl alcohol. In this paper, we are presenting the results of our studies on both the unsaturated alcohols—allyl and propargyl alcohols—and comparing the same with those obtained in the case of acids.

In the case of alkenes and allyl cyanide, the photodissociation leading to allyl radical is thought to proceed from the vibrationally hot ground state formed via internal conversion from the initially populated excited state.[2,3] In both allyl halides and alcohols, the emission spectroscopy studies as well as theoretical calculations on the excited states indicate that the dissociation proceeds via an electronic curve crossing, or by a predissociation mechanism.[1,4] However, Shimo et al.[2] reported a lower yield of allyl radical from photolysis of allyl alcohol as compared to that from allyl chloride, at 193 nm. In a recent study, Morton et al.[1] identified four significant primary dissociation channels, including two different channels leading to Cl atom formation with different kinetic energies (fast and slow), in the photodissociation of allyl chloride at 193 nm. Further, the range of internal energy of the allyl fragments and all the secondary reactions that could take place from these fragments were also discussed in detail. Similar information on the dynamics and

* Corresponding author. E-mail: rdsaini@apsara.barc.ernet.in.

10.1021/jp047657h CCC: $27.50 
Published on Web 08/28/2004

energetics of the dissociation of allyl alcohol was not available. The present study on the energy partitioning between the fragments of allyl alcohol provides this information, which may help in understanding the mechanistic difference between the photodissociations of allyl halide and allyl alcohol, leading to a higher yield of allyl radicals in the chloride.

Propargyl radicals, which are readily formed by photolysis of propargyl compounds,[5] are important intermediates in hydrocarbon reaction systems pertinent to low temperature of planetary systems as well as high temperature of combustion systems. Propargyl compounds have a strong absorption band,[6] attributed to $\pi-\pi^*$ transition, in the 190−200 nm region, with a high absorption cross section ($\sigma$) on the order of $10^{-16}$ cm$^2$ molecule$^{-1}$ as compared to the weaker absorption of allyl compounds ($\sigma = 10^{-19}$ cm$^2$ molecule$^{-1}$) in the same wavelength range.[4] Photodissociation studies of propargyl halides have been carried out by flash photolysis[5] as well as by laser flash photolysis at 193 and 248 nm,[6] and the optical absorption spectrum of the resultant propargyl radical has been characterized. However, to our knowledge, the present work is the first report on the dynamics or energy partitioning during the dissociation of propargyl compounds.

## Experiments

The details of the laser photolysis−laser-induced fluorescence (LP−LIF) setup used in the present work are described elsewhere.[11] Briefly, the photolysis excimer laser (Lambda Physik model Compex-102, Fluorine version) and the probe laser (Quantel dye laser with frequency doubling module, model TDL90, pumped by a Quantel seeded Nd:YAG laser, model YG980E−20) intersect at the center of the reaction cell. Induced fluorescence from this intersection volume is collected with a lens of 50 mm focal length and detected by the PMT (Hamamatsu, model R928P), which is mounted perpendicular to both the beams. A band-pass filter (with $\lambda_{center} = 310$ nm, fwhm = 20 nm, % $T_{310\ nm} = 10$) is used between the collecting lens and PMT to cut off the scattering from the photolysis laser. In addition, baffles are used in the sidearms of the cell, and the windows are fixed at the Brewster angle to minimize scattering. A PC controls the wavelength scan of the dye laser and acquisition of the data after the signals are integrated and averaged by a boxcar integrator, SRS 250. A delay generator controls the time delay between the photolysis and the probe laser beams. Both the pump and probe laser beams were unfocused and their intensities were monitored by photodiodes to correct for any fluctuations. The intensity of the excimer laser was kept very low (<0.5 mJ cm$^{-2}$) to avoid any biphotonic processes. The signal was found to be linear with pump and probe laser intensities as well as with pressure of the sample. The laser frequency was calibrated using an optogalvanic cell (Fe−Ne).

Propargyl and allyl alcohols (Merck, >99%) were used directly. Low pressure (20−40 mTorr) of the sample was maintained in a flow cell, and it was measured by a capacitance gauge (Pfeiffer Vacuum, model CMR 263).

## Results

**A. Rotational Energy Distribution.** In the present study, the $A^2\Sigma(v' = 0) - X^2\Pi(v'' = 0)$ and $A^2\Sigma(v' = 1) - X^2\Pi(v'' = 1)$ transitions were probed by LIF. A portion of the typical LIF spectrum of OH radicals from propargyl alcohol is given in Figure 1 with appropriate assignments.[12] The transitions corresponding to $\Delta N = -1, 0, +1$ are represented by P, Q, and R branches, respectively. The relative populations of the

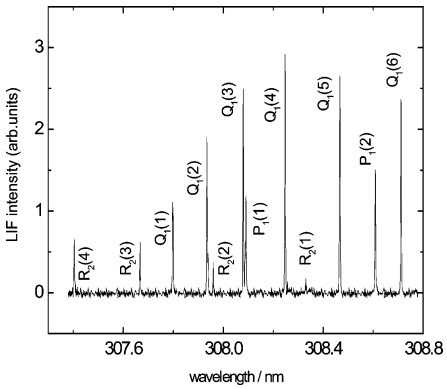


**Figure 1.** Portion of the LIF excitation spectrum of OH radical with proper assignments of rotational lines, measured after photolysis of propargyl alcohol at 193 nm. Pressure of propargyl alcohol = 25 mTorr; intensity of the pump laser = 0.2 mJ cm$^{-2}$; delay = 100 ns.

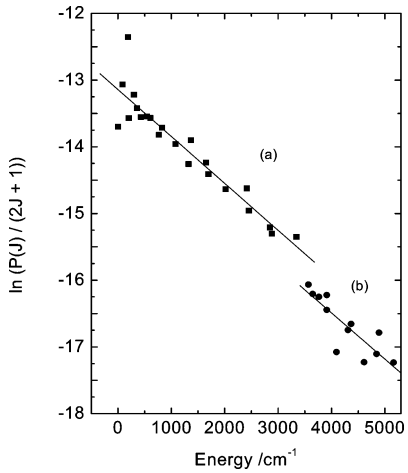


**Figure 2.** Typical Boltzman plots of the distribution of rotational energy in the nascent OH radical from allyl alcohol: (a) $v'' = 0$ and (b) $v'' = 1$ vibrational levels.

OH fragments in different rotational states are calculated by analyzing the different rotational lines. The P and R lines probe the $\Pi^+(A')$ state, whereas Q lines probe the $\Pi^-(A'')$ state. The Doppler broadened LIF signals were fitted with a Gaussian function and the areas under the fitted curves were considered as their LIF intensities for the subsequent calculations. For different lines, the LIF signal intensities thus obtained were further normalized with respect to photolysis laser intensity, probe laser intensity and Einstein's absorption coefficient, $B_{ij}$.[13] Typical Boltzman plots based on this normalized population distribution are shown in Figure 2 for allyl alcohol. From the slopes of these plots, the rotational temperatures of $v'' = 0$ and $v'' = 1$ states are calculated. After several such measurements, the average rotational temperature of OH radical ($v'' = 0$) is found to be 1960 ± 150 K. Similarly for propargyl alcohol, the average rotational temperature is 1760 ± 130 K (Figure 3). From similar analysis of the measured LIF intensities, the population distributions of OH radicals in the higher vibrational state ($v'' = 1$) are found to be characterized by the average rotational temperatures of 1900 ± 250 and 690 ± 120 K for allyl and propargyl alcohols, respectively. Our values for allyl alcohol are in agreement with the average rotational energies measured by Kang et al.,[10] viz., 2050 K (1430 ± 110 cm$^{-1}$) and 1900 K (1320 ± 60 cm$^{-1}$) for $v'' = 0$ and 1, respectively.

**B. Vibrational Energy Distribution.** The population ratio of the corresponding rotational lines in the $v'' = 0$ and $v'' = 1$ vibrational states is used to calculate the average vibrational

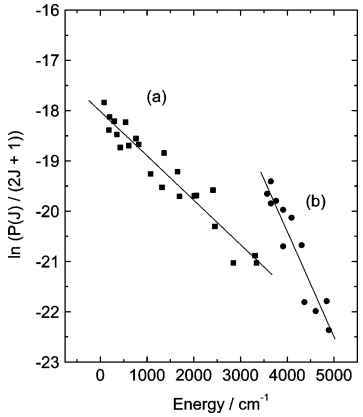


**Figure 3.** Typical Boltzman plots of the distribution of rotational energy in the nascent OH radical from propargyl alcohol: (a) $v = 0$ and (b) $v = 1$ vibrational levels.

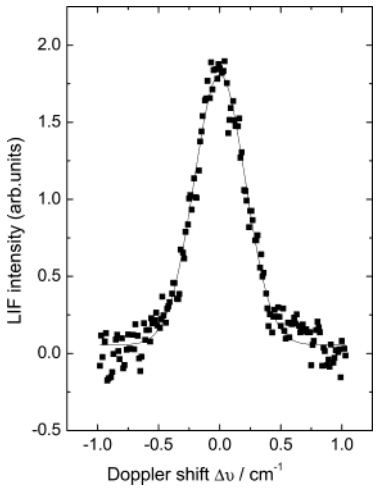


**Figure 4.** Observed Doppler broadened rotational line, $P_1(2)$, of OH from propargyl alcohol, fitted by a Gaussian function.

temperature of the OH radicals. If we consider the $P_1(2)$ lines in both the (0,0) and (1,1) vibronic transition, the vibrational temperature can be calculated from the following Boltzmann equation

$$P(P_1(2);\, v'' = 1)/P(P_1(2);\, v'' = 0) = \exp(-\Delta\epsilon_v\, hc/kT_V)$$

where the right-hand side of the equation represents the intensity ratio of $P_1(2)$ lines of both (0,0) and (1,1) vibrational bands, $\Delta\epsilon_v$ is the energy difference between $v'' = 1$ and $v'' = 0$ for a given spin−orbit state, and $T_V$ is the vibrational temperature. The average vibrational temperatures obtained from all the common lines in 0−0 and 1−1 transitions are 2070 ± 380 K for allyl alcohol, and 2130 ± 440 K for propargyl alcohol. From the vibrational temperature, the mean vibrational energies of OH can be calculated as $\Delta\epsilon_v/(\exp(\Delta\epsilon_v/kT_v) - 1)$. The vibrational energies calculated from the above temperatures are 3.6 ± 1.6 and 4.0 ± 1.8 kJ mol$^{-1}$ for allyl and propargyl alcohols, respectively. This vibrational energy corresponds to the relative populations of 0.92 and 0.08 in $v'' = 0$ and 1 respectively for both allyl and propargyl alcohols.

**C. Translational Energy Distribution.** The Doppler profile of the $P_1(2)$ line of OH from propargyl alcohol is given in Figure 4. The normalized Doppler profile fits into a Gaussian function. This was corrected for the laser profile, which is another Gaussian function with a bandwidth of 0.07 cm$^{-1}$. The corrected Doppler profile reflects the distribution of the velocity component, $v_z$, of the OH radicals along the direction of propagation of the probe laser beam due to the linear Doppler shift $\Delta\nu = (\nu - \nu_0) = v_z\nu_0/c$. Assuming that the velocity distribution is isotropic, the average translational energy in the laboratory frame ($E_T^{lab}$ (OH)) can be calculated as $^3/_2(m_{OH}v_z^2)$, where $v_z$ represents the average velocity of the OH radical, calculated from the Doppler width using the above relation. In the case of allyl alcohol, Kang et al.[10] obtained identical signals in two different experimental geometries, monitoring the OH radicals in two perpendicular directions. This justifies the assumption of isotropic distribution. The translational energy is found to be independent of the rotational excitation. Thus, the average translational energy of OH fragments in the laboratory frame is calculated to be 84.6 ± 15.5 kJ mol$^{-1}$ in the case of allyl alcohol and 104.4 ± 15.8 kJ mol$^{-1}$ in the case of propargyl alcohol. From these values, considering the conservation of momentum, the average relative translational energies of both the fragments are calculated to be 118.4 ± 22.2 and 148.1 ± 22.6 kJ mol$^{-1}$ for allyl and propargyl alcohols, respectively. The temporal profile for OH radical build-up was monitored for different rotational lines of the ground vibrational state of the OH radical. The formation of OH radical was found to be complete within the laser pulse time, i.e., a few nanoseconds.

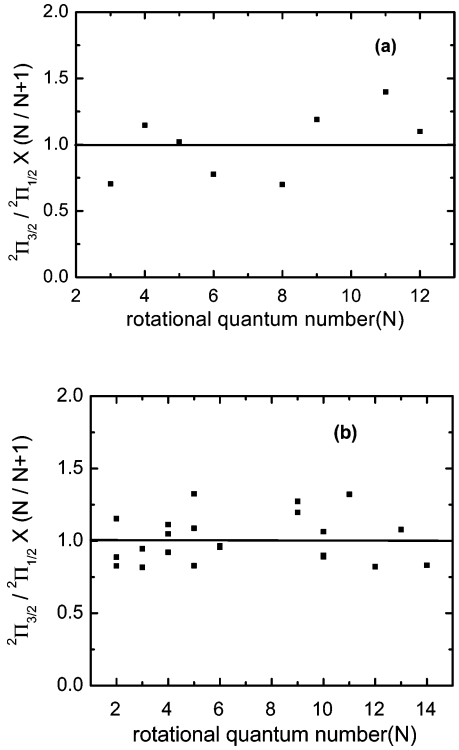


**Figure 5.** Spin−orbit ratio as a function of rotational quantum number ($N$) of OH: (a) in allyl alcohol and (b) in propargyl alcohol.

**D. Spin—Orbit and Λ-Doublet-State Distributions.** The spin−orbit ratios, obtained from the measured $\Pi_{3/2}/\Pi_{1/2}$ ratios after multiplying by the appropriate statistical weights, are plotted against the rotational quantum number ($N$) of OH in Figure 5. The average value is one, thereby indicating a statistical distribution, without any preference for either of the spin−orbit ($J$) states in the dissociation process. The Λ doublet distributions, i.e., the ratio of $^2\Pi$ (A″) and $^2\Pi$(A′) states, obtained from the population ratio of Q and P/R lines are given in Figure 6. The relative population of the Λ doublets provides a clue on the exit channel dynamics in the dissociation step. In the present case, this ratio is less than 1, i.e., nonstatistical for both allyl and propargyl alcohols.

**TABLE 1: Partitioning of Available Energy ($E_{avl}$) into Various Modes in the Photofragments of Allyl and Propargyl Alcohols at 193 nm[d]**

| | | available energy | translational energy (total) | rotational energy of OH radical | vibrational energy of OH radical | internal energy of fragment R |
|---|---|---|---|---|---|---|
| allyl alcohol | | 298.7 | | | | |
| | experimental | | 118.4 ± 22.2 (0.40) | 16.3 ± 1.3 (0.05) | 3.6 ± 1.6 (0.01) | 160.3 (0.54) |
| | statistical | | 30.1(0.10) | 9.4 (0.03) | 5.9 (0.02) | 253.0(0.85) |
| | impulsive | | 171.4(0.57) | 6.4(0.02) | 0.43(≪0.01) | 120.5 (0.41) |
| | hybrid[a] | | 118.5 | 6.1 | 2.8 | 170.4 |
| | literature[10] | | 98.8 | 17.0[c] | 5.3[c] | |
| propargyl alcohol | | 307.8 | | | | |
| | experimental | | 148 ± 23 (0.48) | 13.8 ± 1.0 (0.04) | 4.0 ± 1.8 (0.01) | 142.0 (0.46) |
| | statistical | | 38.0 (0.12) | 13.2(0.04) | 9.8(0.03) | 246.5(0.8) |
| | impulsive | | 179.2 (0.58) | 6.6 (0.02) | 0.5 (<0.01) | 121.3 (0.40) |
| | hybrid[b] | | 148.7 | 7.3 | 3.8 | 147.5 |

[a] Calculated with a barrier of 95.5 kJ mol$^{-1}$, assuming its complete transfer to the product translation. [b] Similar to footnote a, with a barrier of 123.0 kJ mol$^{-1}$. [c] Calculated from the reported[10] average rotational energy of 1430 and 1320 cm$^{-1}$ and from the ratio of vibrational populations 0.89/0.11 for $v = 0/v = 1$. [d] All energies are given in kJ mol$^{-1}$ and the values given in parantheses correspond to the fractions of available energy going to the particular mode, either experimental or calculated.

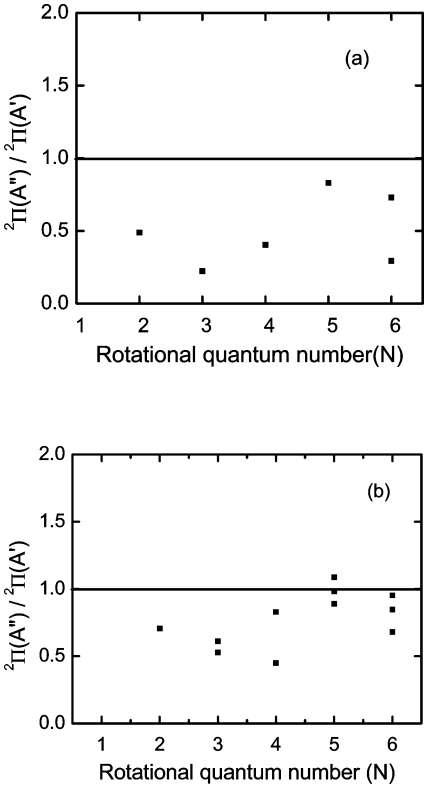


**Figure 6.** Λ-doublet ratio as a function of rotational quantum number ($N$) of OH: (a) in allyl alcohol and (b) in propargyl alcohol.

## Discussion

**Available Energy.** The C−OH bond dissociation energies for both these alcohols can be calculated from the known enthalpy of formation of the radicals and the parent compounds.

$$CH_2{=}CH{-}CH_2{-}OH \rightarrow CH_2{=}CH{-}CH_2^{\bullet} + {}^{\bullet}OH \quad (1)$$

$$CH{\equiv}C{-}CH_2OH \rightarrow CH{\equiv}C{-}CH_2^{\bullet} + {}^{\bullet}OH \quad (2)$$

The enthalpies of formation of allyl[14] and propargyl radicals[15] are 170.7 and 340.6 kJ mol$^{-1}$, respectively. Though allyl alcohol has different conformers with rotational barriers about C−C and C−O bonds, only two rotomers are predominant at room temperature,[16] and the reported enthalpy of formation of allyl alcohol is −124.5 kJ mol$^{-1}$, at room temperature.[17] The enthalpy of formation of OH radical[15] is 39.3 kJ mol$^{-1}$. Thus, the C−OH bond dissociation energy, the $\Delta H$ of reaction 1, is calculated to be 334.5 kJ mol$^{-1}$. In the case of propargyl alcohol, there are two isomers, designated as cis and trans, with O−H rotational barriers in the C−C−O−H plane. Their enthalpies of formation are calculated theoretically as 55.3 and 60.3 kJ mol$^{-1}$ respectively.[18] Considering that 90% cis form and 10% trans form will be present at room temperature, the weighted average value of the C−OH bond dissociation energy, $\Delta H$ of reaction 2, is calculated to be 324.1 kJ mol$^{-1}$.

Other channels, such as C−H, O−H and C−C bond dissociations are also possible for these unsaturated alcohols. In allyl alcohol, the reported C−H bond strength is 341 kJ mol$^{-1}$.[15] The C−C bond dissociation energies, calculated from the reported heats of formations of $CH_2OH$, CH2═CH and CH≡C radicals,[17] are 406.7 and 492.5 kJ mol$^{-1}$ for allyl and propargyl alcohols, respectively. The O−H bond dissociation energies of alcohols are generally higher than 400 kJ mol$^{-1}$. Thus, it appears that, in both these molecules, the C−OH dissociation is the lowest energy channel, though not very different from the C−H bond dissociation. The energy of 193 nm photon is 620 kJ mol$^{-1}$, sufficient to break these bonds. The available excess energy ($E_{avl}$) after C−OH dissociation is calculated as the energy of 193 nm photon − the C−OH bond dissociation energy + the internal energy of the parent molecule at room temperature (see Table 1).

**Energy Partitioning.** The available excess energy ($E_{avl}$) appears in different forms, as translational, rotational and vibrational energies of the fragments and the observed energy distribution is given in Table 1. The measured rotational and vibrational energies, as presented here, of the OH radicals from the photodissociation of allyl alcohol are largely in agreement with those of Kang et al.[10] The translational energy observed in the present case, though marginally higher, is comparable with their observation within experimental error. The fraction of available energy that goes into translation ($f_T$) is found to be higher in propargyl alcohol as compared to that in allyl alcohol. Correspondingly, a marginally higher fraction of available energy is deposited as the internal energy in the fragments of allyl alcohol.

There can be different mechanisms of depositing the excess energy in the fragments. For example, the rotation of the parent molecule can be transferred to the fragments. However in the present case, considering the moment of inertia of the parent ground state and that of the OH radical, an approximate

calculation[19] shows that the contribution from this source will be very small. The parent molecule's bending or torsional vibrational motion associated with the C−OH bond, which disappears on dissociation, can be transferred to the fragments' rotational energy. During the dissociation of both these molecules, five vibrational modes are lost whose energy may appear as the rotational energy of the fragments. In addition, rotational energy can arise from the torque imparted to the separating fragments at the instant of dissociation. The products' vibrational energy arises from the vibrational energy of the parent compound at the time of the dissociation. Besides, a part of the excess energy would be transferred as relative translational energy to the two fragments trying to separate under a repulsive force. The observed energy distribution among the fragments in these three different modes deviate markedly, both qualitatively and quantitatively, from that calculated according to pure statistical[20] and soft impulsive[21] models, as shown in Table 1. The geometries of the ground states of allyl and propargyl alcohols, and those of photofragments were calculated using Gaussian-92 at HF/6-311++G(d,p) level to determine all the required parameters. The large deviation of the energy distribution among fragments from the statistical model indicates that the dissociation is probably taking place from an excited-state potential energy surface.

**Origin of Fragment Excitation and Hybrid Model.** The fragments correlate directly with the geometry of the parent molecule at the instant of dissociation, which may be different from that in the ground state. In this context, it is interesting to see the results of Parsons et al.,[4] who studied the excited state of allyl alcohol populated at 199.7 nm, by emission spectroscopy as well as by ab initio calculations. Their calculations showed that in both the conformers present at room temperature, the excited-state populated by 199.7 nm had a major contribution from the $\pi_{C\bullet-\bullet C}\ \pi^*_{C\bullet-\bullet C}$ state along with a minor contribution from a state of $\pi \rightarrow$ Rydberg character. This conclusion is supported by the experimental emission spectra, which show maximum intensity in C═C stretch along with some torsional motion. In addition, the emission spectrum of allyl alcohol shows peaks due to O−H stretch and $CH_2$ rock modes. This implies that part of the energy is already distributed in the internal modes from the Franck−Condon excited state. The above study shows that the initially prepared excited state has neither a contribution from the repulsive n-$\sigma^*$ state, from which C−OH dissociation is possible, nor enough vibrational energy in the C−O stretching mode to lead to direct dissociation. Thus, the process of dissociation must necessarily involve curve crossing to another excited state or to the ground state, which can lead to dissociation. It is also clear that there is a partial energy redistribution before the molecule reaches or crosses over to the dissociative state. This type of dissociation which involves a partial randomization before an impulsive bond breaking is described by Chang et al.,[22] and the model proposed is known as the hybrid model.

In the hybrid model, the molecule has an exit barrier in the dissociation channel so that the excess energy beyond the barrier is partitioned statistically and the barrier energy goes impulsively between the two fragments governed by the conservation of linear and angular momenta. Such a barrier can arise due to interaction between the initial and the final excited states. Further, a modified impulsive model using rigid rotor approximation (which considers partitioning only between translational and rotational energies of the two fragments) was used to calculate the distribution of energy released by the exit barrier. These energies are added to the respective translational and rotational energies arising from the statistical distribution of the excess energy above the barrier, to obtain the final energy distribution. The presence of such a barrier also implies that the dissociation does not occur from the ground state, because the recombination of the fragments generally does not have any barrier. Thus, dissociation must be taking place from an excited triplet or singlet state, which is reached after electronic curve crossing.

In the case of allyl alcohol, Kang et al.[10] have considered this model and predicted a barrier of 70 kJ $mol^{-1}$ (5800 $cm^{-1}$), assuming that all the exit barrier energy goes as translational energy. If we make a similar assumption, the observed translational energies in the present experiments are possible with barriers of 95.5 and 123 kJ $mol^{-1}$, for allyl and propargyl alcohols respectively, as shown in Table 1. However, the error in the predicted rotational energy is very large for both the molecules. Obviously, the assumption of exit barrier energy being wholly converted to translational energy is not correct. According to hybrid model,[22] the partitioning of barrier energy between the translational and rotational modes of the fragments can be calculated by the following equations

$$E_R^{\text{imp}}(\text{A}) = E_T^{\text{imp}} b_A^2 \mu_{AB}/I_A$$

$$E_R^{\text{imp}}(\text{B}) = E_T^{\text{imp}} b_B^2 \mu_{AB}/I_B$$

where $E_T^{\text{imp}}$ is the translational energy of the two fragments A and B given by $E^{\text{imp}}/[1+ (b_A^2\mu_{AB}/I_A) + (b_B^2\mu_{AB}/I_B)]$, $E^{\text{imp}}$ is the barrier energy which is distributed impulsively, $\mu_{AB}$ is the reduced mass, $b_{\text{frag}}$ is the impact parameter of the fragment, and $I_{\text{frag}}$ is the moment of inertia of the fragments about an axis through the center of mass of the respective fragment, perpendicular to the plane containing the center of mass and the two separating atoms. The impact parameter $b_{\text{frag}}$ is given by $r$ sin $\chi_{\text{frag}}$, where $r$ is the distance from the dissociating atom to the center of mass of the corresponding fragment and $\chi_{\text{frag}}$ is the angle between the bond to be broken and a line from the center of mass of the fragment to the atom which is getting separated. Thus, prediction of energy distribution among the different modes in the fragments requires the knowledge of transition state geometry as well as the barrier height, which could not be determined for both allyl and propargyl alcohols. However, the large fraction of rotational energy of the OH fragments from allyl alcohol can be explained only by either a drastic change in the transition state geometry as compared to the parent molecule or by the rotational energy originating from other sources, such as disappearing bending modes on dissociation of the parent molecule. If the bond angle, ∠C−O−H changes toward 90° and ∠C−C−O changes toward 180° (i.e., OH moving to the same plane as that of C═C−C), there will be a considerable increase in the fraction of rotational energy going to the O−H fragment. Accurate calculations on the excited state potential energy surfaces and transition state are very essential to clearly understand the details of energy partitioning among the fragments.

**Comparison with Propargyl Alcohol.** One of the main objectives of this work is to compare the energy partitioning in the two unsaturated alcohols. As discussed earlier, there is a definite, though small, difference between the energy distributions in the fragments of allyl and propargyl alcohols. More translational energy goes to the fragments of propargyl alcohol and more internal energy goes to the fragments, in particular the O−H fragment, of allyl alcohol. Since the energy partitioning among the products deviates significantly from the statistical model, this cannot be attributed to the presence of a larger

number of vibrational modes in allyl alcohol/allyl radical. Moreover, the rotational energy of OH fragments is significantly different in these two cases. The rotational temperatures of ground and first vibrational states of OH radicals as well as its vibrational temperature are almost the same in the case of allyl alcohol (1960, 1900, and 2070 K respectively) whereas they are found to be different (1760, 690, and 2130 K) in the case of propargyl alcohol. Therefore, the observed difference in the pattern of energy distribution may be the effect of a number of factors as discussed below.

The energy barrier in the case of propargyl alcohol may be much higher than that in allyl alcohol, giving more translational energy. Or even if the barrier energies are comparable, the fraction of energy from the release of the barrier going to translational mode in propargyl alcohol is higher and that going to rotational mode is lower than that in allyl alcohol, due to very different transition state geometries. The linear geometry of the propargyl radical and the angle at which the impulse is given to the radical at the time of dissociation may play a role in deciding these factors. In the ground state of propargyl alcohol, the conformation with O−H group oriented toward the C≡C bond is preferred. In allyl alcohol also, theoretical calculations and microwave spectroscopic evidence show that the two stable conformers are those with O−H oriented toward the C═C bond, though the C−C−C−O skeleton is nonplanar. Stability of such conformers of allyl and substituted allyl alcohols are attributed to a weak hydrogen bonding between the $\pi$ bond and the hydrogen atom,[23] though spectroscopic evidence for such interaction is obtained only in longer chain unsaturated alcohols with more than three carbon atoms.[24] If such an interaction is possible, it may be present even in the first $\pi-\pi^*$ excited state of propargyl alcohol, whereas in the excited state of allyl alcohol, this will be vanishing. Such an interaction may introduce constraints on the transition state geometry of propargyl alcohol.

Although there is no direct experimental evidence from literature, the similarity of the results on vibrational excitation of OH fragment between allyl and propargyl alcohols suggests that the O−H vibration is excited along with the electronic excitation in the case of propargyl alcohol too. However, there is a significant difference in their internal energy distribution. Almost equal vibrational and rotational temperatures in $v'' = 0$ and $v'' = 1$ states in the OH fragments from allyl alcohol may be indicative of a localized equilibration of energy in the internal modes at some stage of the dissociation process. Such a process is absent in the case of propargyl alcohol, as suggested by different rotational and vibrational temperatures.

It is interesting to note that the relative $f_T$ values in allyl and propargyl alcohols are qualitatively in agreement with those in the corresponding double and triple bonded carboxylic acids, namely acrylic and propiolic acid. The $f_T$ value in the triple bonded molecule is greater than that in the double bonded molecule. However the quantitative difference in the carboxylic acids is much higher, with $f_T = 0.25$ and 0.75 in acrylic[7] and propiolic[8] acids, respectively.

**Spin—Orbit and Λ-Doublet Ratios.** In most of the cases where spin preference is observed, it has been difficult to understand the origin for this preference, although in some cases it is assigned to a coupling of the initially populated state to a nearby triplet state.[26] However, in many cases, including acetic acid[11,26] and pyruvic acid,[27] though the results of theoretical calculations had indicated a transition state from the excited triplet state, such a spin preference was not experimentally observed. Accordingly, the absence of spin preference observed in the present studies does not necessarily rule out the possibility of dissociation from the triplet states of allyl and propargyl alcohols.

A nonstatistical population distribution of Λ-doublets at high $J$ values in the $^2\Pi$ electronic state of the fragment is indicative of a molecular process proceeding through a planar intermediate.[25] However, in the present case there is a preferential population of P and R states even at lower $J$ values, which remains more or less unchanged until $N = 6$. This trend is more pronounced in allyl alcohol.

The present results are in disagreement with the observation of Kang et al.,[10] that the spin−orbit ratio is nonstatistical and Λ doublet ratio is statistical in allyl alcohol. The reason for this difference is not understood.

Unlike alkenes, both unsaturated alcohols and halides are considered to undergo dissociation from the excited states, with a minor C−Cl dissociation channel (3%) from the ground state, in the case of allyl chloride.[1] However, the earlier flash photolysis studies show that the yield of allyl radical upon 193 nm photolysis is about four times higher for chloride as compared to alcohol. (The ratio of the yield of allyl radical from allyl chloride with respect to that from propene is 1 where as the similar ratio is only 0.23 for allyl alcohol.[2]) This could be either because of lower quantum yield for the primary dissociation channel leading to allyl and OH fragments or due to fast secondary reactions of allyl radical, which reduces its concentration at the time of observation (200 ns after 193 nm laser pulse) in allyl alcohol. So far there is no measurement of the quantum yield of OH fragments, which could have confirmed one of the above possibilities. The extent of secondary reactions of the allyl radicals will depend on the internal energy of the nascent radical. The available energy after photon absorption and primary bond dissociation is higher in allyl chloride (321.3 kJ $mol^{-1}$) as compared to that in allyl alcohol (see Table 1). A total of 97% of the C−Cl bond fission events occur from the excited-state surface leading to allyl radicals with a range of internal energies that span 66.9−237.6 kJ $mol^{-1}$ (plus parent internal energy), which are found to be stable to dissociation.[1] C−H bond dissociation to give allene or isomerization to 2-propenyl radical can take place only if the nascent allyl radical is formed with an internal energy higher than 251 kJ $mol^{-1}$ in the ground electronic state.[28] A possible C−C bond dissociation channel was also not indicated in this energy range.[1] In the present work, we have measured the total average translational energy and internal energy of the OH fragment after the primary dissociation step. From this, the average internal energy left with allyl radical is estimated to be 160.3 kJ $mol^{-1}$, which is not very different from the average energy of allyl radical from allyl chloride. Hence, it does not appear that the large difference in the yield of allyl radical in the two cases is due to the increased secondary dissociation in the case of allyl alcohol. Our investigations did not give any evidence of a strong fluorescence or phosphorescence from the excited states formed by absorption of 193 nm light. Thus, the reduced yield of allyl radical in allyl alcohol, as compared to allyl chloride, can be explained by a higher contribution of other competing primary dissociation channels in the former. Theoretical calculations and emission spectrum of the dissociative excited state of allyl chloride at 199 nm suggest a significant admixture of $\sigma^*_{C-Cl}$ character in the $\pi-\pi^*$ state, even in the Franck−Condon region for the excitation of allyl chloride. As mentioned earlier in the discussion, similar studies in the case of allyl alcohol do not indicate any such mixing of $\sigma^*_{C-Cl}$ character in its $\pi-\pi^*$ state. Probably, this could be the reason for C−X bond scission to

be the predominant primary dissociation channel in allyl chloride (X = Cl), whereas the same could be only one of the major channels in allyl alcohol (X = OH). Since there is only a single relative yield measurement,[2] further quantitative studies on different primary dissociation channels of allyl alcohol, to substantiate this observation, will be of interest.

## Summary

The dynamics of C−OH bond dissociation in allyl and propargyl alcohols have been studied by measuring the energy distribution in the product, OH radical, employing the LIF technique. The relative translational energies of the fragments are 118.4 ± 22.2 ($f_T = 0.4$) and 148 ± 23 kJ mol$^{-1}$($f_T = 0.5$) for allyl and propargyl alcohols, respectively. The observed energy distribution in the photofragments of allyl alcohol is very similar to the recent observations by Kang et al.[10] except for a marginally higher translational energy. The nonstatistical as well as nonimpulsive distribution of energy in different modes suggests the existence of an exit barrier in the excited states of both the unsaturated alcohols. There is an observable and definite difference in the relative energy distribution within the fragments of these double and triple bonded alcohols, though not as pronounced as in the case of corresponding carboxylic acids, namely acrylic and propiolic acids. In allyl alcohol, a higher fraction of energy goes into internal modes of the fragments, especially rotational mode of OH, whereas the fraction of energy that goes into translational mode is higher in propargyl alcohol. This suggests a difference in the transition state geometries of the two molecules, probably due to $\pi$−H interactions in propargyl alcohol. In addition, the vibrational temperature and the rotational temperatures of both vibrational states ($v'' = 0$ and 1) are the same in the OH fragments of allyl alcohol (2070, 1960, and 1900 K, respectively), suggesting a partial equilibration, whereas they are all different in propargyl alcohol (2130, 1760, and 690 K, respectively). The present observations call for the advanced calculations on the excited-state potential energy surfaces and transition state geometries of allyl and propargyl alcohols.

**Acknowledgment.** The authors are grateful to Dr. P. N. Bajaj and Dr. T. Mukherjee for their keen interest during the course of this work.

## References and Notes

(1) Morton, M. L.; Butler, L. J.; Stephenson, T. A.; Qi, F. *J. Chem. Phys.* **2002**, *116*, 2763.

(2) Shimo, N.; Nakashima, N.; Ikeda, N.; Yoshihara, K. *J. Photochem.* **1986**, *33*, 279; Nakashima, N.; Shimo, N.; Ikeda, N.; Yoshihara, K. *J. Phys. Chem.* **1984**, *88*, 5803.

(3) Oh, C. Y.; Shin, S. K.; Kim, H. L.; Park, C. R. *Chem. Phys. Lett.* **2001**, *342*, 27.

(4) Parsons, B. F.; Szpunar, D. E.; Butler, L. J. *J. Phys. Chem.* **2000**, *104*, 10669.

(5) Fahr, A.; Hassanzadeh, P.; Laszlo, B.; Huie, R. E. *Chem. Phys.* **1997**, *215*, 59.

(6) Ramsay, D. A.; Thistlethwaite, P. *Can. J. Phys.* **1966**, *44*, 1381.

(7) Upadhyaya, H. P.; Kumar, A.; Naik, P. D.; Sapre, A. V.; Mittal, J. P. *J. Chem. Phys.* **2002**, *117*, 10097.

(8) Kumar, A.; Upadhyaya, H. P.; Naik, P. D.; Maity, D. K.; Mittal, J. P. *J. Phys. Chem.* **2002**, *106*, 11847.

(9) Kumar, A.; Dhanya, S.; Upadhyaya, H. P.; Naik, P. D.; Saini, R. D. *Book of Abstracts*; National Symposium on Radiation and Photochemistry, Kanpur, India, March 3−5, 2003; Indian Society for Radiation and Photochemical Sciences, BARC: Mumbai, India, 2003; p 41.

(10) Kang, T. Y.; Shin, S. K.; Kim, H. L. *J. Phys. Chem. A* **2003**, *107*, 10888.

(11) Naik, P. D.; Upadhyaya, H. P.; Kumar, A.; Sapre, A. V.; Mittal, J. P. *Chem. Phys. Lett.* **2001**, *340*, 116.

(12) Dieke, G. H.; Crosswhite, H. M. *J. Quant. Spectrosc. Radiat. Trans.* **1961**, *2*, 97.

(13) Chidsey, I. L.; Crosley, D. R. *J. Quant. Spectrosc. Radiat. Trans.* **1980**, *23*, 187.

(14) Berkowitz, J.; Ellison, G. B.; Gutman, D. *J. Phys. Chem.* **1994**, *98*, 2744.

(15) McMillan, D. F.; Golden, D. M. *Annu. Rev. Phys. Chem.* **1982**, *33*, 493.

(16) Vanhouteghem, Pyckhout, W.; Van Alsenoy, C.; Van den Enden, L. *J. Mol. Struct.* **1986**, *140*, 33.

(17) *CRC Handbook of Chemistry and Physics*, 80th ed.; Lide, R., Ed.; CRC Press: Boca Raton, FL, 1999.

(18) Melius, C. F. *BACMP4 Heats of formation data file, version 16*; Sandia National Laboratories: Albuquerque, NM, 1996.

(19) Hanazaki, I. *Chem. Phys. Lett.* **1994**, *218*, 151.

(20) Tuck, A. F. *J. Chem. Soc., Faraday Trans. I* **1977**, *73*, 689.

(21) Galloway, D. B.; Glenewinkel-Meyer, T.; Bartz, J. A.; Huey, L. G.; Crim, F. F. *J. Chem. Phys.* **1994**, *100*, 1946.

(22) Chang, A. H. H.; Hwang, D. W.; Yang, X. M.; Mebel, A. M.; Lin, S. H.; Lee, Y. T. *J. Chem. Phys.* **1999**, *110*, 10810.

(23) Leonov, A.; Marstokk, K.-M.; de Meijere, A.; Møllendal, H. *J. Phys. Chem. A* **2000**, *104*, 4421.

(24) Kowski, K.; Lutleke, W.; Rademacher, P. *J. Mol. Struct.* **2001**, *567*−*568*, 231.

(25) Vasudev, R.; Zare, R. N.; Dixon, R. N. *J. Chem. Phys.* **1984**, *80*, 4863.

(26) Naik, P. D.; Upadhyaya, H. P.; Kumar, A.; Sapre, A. V.; Mittal, J. P. *J. Photochem. Photobiol. C, Photochem. Rev.* **2003**, *3*, 165.

(27) Dhanya, S.; Maity, D. K.; Upadhyaya, H. P.; Awadhesh Kumar, N. P. D.; Saini, R. D. *J. Chem. Phys.* **2003**, *118*, 10093.

(28) Davies, S. G.; Law, C. K.; Wang, H. *J. Phys. Chem. A* **1999**, *103*, 5889.